



Cholera in Haiti: Reproductive numbers and vaccination coverage estimates

Zindoga Mukandavire¹, David L. Smith^{2,3} & J. Glenn Morris Jr¹

¹Emerging Pathogens Institute, University of Florida, Gainesville, Florida, Gainesville, FL 32610, USA, ²Department of Epidemiology, Johns Hopkins Bloomberg School of Public Health, Baltimore, MD, USA, ³Fogarty International Center, National Institutes of Health, Bethesda, MD, USA.

SUBJECT AREAS:
BACTERIAL INFECTION
DIFFERENTIAL EQUATIONS
APPLIED MATHEMATICS
POPULATION DYNAMICS

Received
12 March 2012

Accepted
29 November 2012

Published
10 January 2013

Correspondence and
requests for materials
should be addressed to
Z.M. (zmukandavire@
gmail.com)

Cholera reappeared in Haiti in October, 2010 after decades of absence. Cases were first detected in Artibonite region and in the ensuing months the disease spread to every department in the country. The rate of increase in the number of cases at the start of epidemics provides valuable information about the basic reproductive number (\mathcal{R}_0). Quantitative analysis of such data gives useful information for planning and evaluating disease control interventions, including vaccination. Using a mathematical model, we fitted data on the cumulative number of reported hospitalized cholera cases in Haiti. \mathcal{R}_0 varied by department, ranging from 1.06 to 2.63. At a national level, 46% vaccination coverage would result in an (\mathcal{R}_0) < 1, which would suppress transmission. In the current debate on the use of cholera vaccines in endemic and non-endemic regions, our results suggest that moderate cholera vaccine coverage would be an important element of disease control in Haiti.

A cholera outbreak was confirmed in Haiti on October 21, 2010 by the National Laboratory of Public Health of the Ministry of Public Health and Population (MSPP). Cholera had not been documented in Haiti for decades, and outbreaks had been thought unlikely after the earthquake on 12 January 2010¹. Cholera was heralded in the Artibonite region, a rural area north of Port-au-Prince, followed in the ensuing months by spread of the disease throughout the country. Spread was facilitated by the earthquake-related disruptions to water and sewage facilities and damage to a local public health infrastructure that was already weak¹. Haiti's populations were immunologically naïve to cholera after its long absence, so the potential for a severe cholera epidemic was high, much like recent cholera epidemics in Zimbabwe and other emerging epidemic-prone regions. Following the initial epidemic wave, there were also concerns about the possibility of cholera establishing long-term endemicity in Haiti, marked by the traditional recurrent seasonal epidemics that are characteristic of the disease.

There is an increasing appreciation of the utility of mathematical models in informing public health policy, both in the emergency situation of an initial cholera epidemic^{2–6} (Table 1), and in long-term public health management of seasonal epidemics. Here, we consider a model that we developed in association with the 2008–2009 Zimbabwe epidemic to explicitly estimate the basic reproductive numbers (\mathcal{R}_0) for the disease, and make public health recommendations on the usefulness of cholera vaccines on a finer scale. In contrast to earlier models applied to the Haitian epidemic, this model permits incorporation of recently recognized differences in transmission pathways for cholera: a “fast,” or “human-to-human” transmission pathway that takes advantage of the lower infectious dose of hyperinfectious *V. cholerae* in freshly passed stool, vs. a “slow” transmission pathway that involves movement between environmental reservoirs and human populations. We also explore the impact of variation in parameter estimates, including estimates for rates of asymptomatic carriage, environmental contamination, and infectious dose from environmental exposure. The Haitian Ministry of Health is currently considering implementation of a national vaccination campaign for cholera. Our results underscore the geographic variability in \mathcal{R}_0 in the initial Haitian epidemic, and the corresponding variability in the needed vaccination coverage for effective disease control.

Results

Table 2 provides estimates of the basic reproductive number (\mathcal{R}_0), and partial reproductive numbers due to “fast” human-to-human transmission (\mathcal{R}_h) and “slow” transmission through the environment (\mathcal{R}_e); it also provides data on the corresponding minimum vaccination coverage needed for a cholera vaccine with an estimated 78% efficacy⁷ for the 10 departments and the country as a whole. The cumulative cholera cases were fit with mathematical models for each department and for the whole country (Figure 1). The results in Table 2 show that

Table 1 | Haiti \mathcal{R}_0 estimates

	Data source	Estimate
Bertuzzo <i>et al.</i> ⁴	MSPP	1.98
Chao <i>et al.</i> ⁵	MSPP	2.60
Chunara <i>et al.</i> ²⁸	MSPP	1.27–3.72 (Before Hurricane Tomas) 1.06–1.73 (After Hurricane Tomas)
Chunara <i>et al.</i> ²⁸	Informal sources (HealthMapp & Twitter)	1.54–6.89 (Before Hurricane Tomas) 1.04–1.51 (After Hurricane Tomas)
Tuite <i>et al.</i> ³	MSPP	2.06–2.78

Artibonite department had the highest \mathcal{R}_0 (2.63) and environmental transmission accounted for most of the transmission ($\approx 97\%$) compared to lower values ($\approx 9\text{--}55\%$) in other departments. Artibonite department was the first to report cholera cases¹ and epidemiological studies have revealed that, the contamination of the Artibonite River and its tributaries (*i.e.* sources of drinking and cooking water for villagers) triggered the epidemic⁸. Thus our estimates support the notation that contamination of drinking water sources sparked the outbreak in Artibonite. These results also show that departments neighboring Artibonite had slightly higher \mathcal{R}_0 values (1.37–1.73) compared to other departments (1.06–1.44), suggesting that it was the epidemic focal point. Our analysis showed that \mathcal{R}_h and \mathcal{R}_e estimates are determined by the time scales of the unfolding epidemic *i.e.* with fast growing epidemic curves giving a higher percentage of \mathcal{R}_h than \mathcal{R}_e and vice-versa. However the inference about the estimates of \mathcal{R}_0 is likely more robust than the estimates of the individual transmission components (*i.e.* \mathcal{R}_e vs. \mathcal{R}_h). Aggregated cholera data for Haiti compared with the department estimates will, on average, overestimate the required country-wide vaccination coverage by about 20% (Table 2). Thus for effective disease control, surveillance and resource allocation there is a need to quantify the magnitude of cholera outbreaks using data on a finer resolution. Analysis of data on a finer grain would likely reveal additional heterogeneities in transmission, but the spatial scales at which it is appropriate to aggregate data for the purposes of planning control interventions remain poorly understood. Since cholera vaccines have different efficacies^{9–12}, we also carried out sensitivity analysis to show possible scenarios that may arise from using different types of vaccines by considering an efficacy range of 50–100%.

The results suggest that a vaccine with 50% efficacy may result in cholera control in most of the departments except for Artibonite, which would require a vaccine with at least 65% efficacy (Table 3). However most of the new-generation cholera vaccines have shown an efficacy more than 65%^{7,9–12} for periods sufficient to contain epidemic cholera (*i.e.* depending on vaccination coverage). But, there

are still concerns that most of the studies on vaccine effectiveness were conducted in cholera endemic areas with some degree of immunity within the population, thus these study results may not hold for Haiti where the population was initially immunologically naïve to the disease^{13,14}.

Mapped \mathcal{R}_0 values illustrate the differences in transmission across Haiti (Figure 2). Reproductive numbers were estimated separately for Port-au-Prince (Table 2), and the part of Ouest that does not include Port-au-Prince, as in the data sets on the MSPP website¹⁵. We also estimated the reproductive number for the whole Ouest department, combining hospitalized cases from both Port-au-Prince and Ouest**, which was used for mapping (Figure 2).

We performed sensitivity analysis using a deterministic version of our model to ascertain the robustness of our \mathcal{R}_0 estimates. We carried out sensitivity analysis of κ (the 50% infectious dose for environmental exposure) and χ (the rate of environmental contamination by cholera infected individuals). On the basis of studies conducted by our group in Lima and Bangladesh, peak environmental counts of *ctx*-positive *V. cholerae* from pristine areas have been found to range from 10^1 to 10^2 cfu/mL^{16,17}; even in areas with heavy sewage contamination, peak environmental counts of *ctx*-positive *V. cholerae* were not observed to exceed 10^6 cfu/mL¹⁶. The infectious dose for media-grown *V. cholerae* ingested by healthy North American volunteers ranges from 10^8 to 10^{11} cfu/mL; this drops to $10^4\text{--}10^8$ when the inoculum is given with bicarbonate or food^{18–20}. In a series of studies conducted at the Center for Vaccine Development, University of Maryland, the “standard” *V. cholerae* inoculum in challenges employing health North American volunteers was 10^6 , administered with bicarbonate²⁰.

In the context of these data, we carried out sensitivity analysis to explore the effects of κ on \mathcal{R}_0 estimates. Results using aggregated data for Haiti are shown in Figure 3, which is a plot of estimated \mathcal{R}_0 and corresponding values of κ . Varying κ in a plausible range of 10^5 to 1.5×10^9 cells/ml, which covers the concentration range of vibrios in sewage-contaminated water and also falls within the range of the

Table 2 | Estimates of \mathcal{R}_e , \mathcal{R}_h , \mathcal{R}_0 and minimum vaccination coverages. Ouest department includes Port-au-Prince and Ouest** hospitalized cases. The population estimates were extracted from <http://www.citypopulation.de/Haiti.html>

Department	Population Size/1000	\mathcal{R}_e	SE	% \mathcal{R}_0	\mathcal{R}_h	SE	% \mathcal{R}_0	\mathcal{R}_0	SE	Vaccination Coverage Resulting in $\mathcal{R}_0 < 1$
Haiti[Country]	9923.24	0.84	7.00×10^{-1}	54.01	0.71	0.29	45.35	1.55	0.41	45.4
Artibonite	1571.02	2.54	2.32×10^{-1}	96.70	0.09	0.06	3.30	2.63	0.18	79.5
Centre	678.63	0.58	4.82×10^{-1}	42.12	0.79	0.24	57.88	1.37	0.24	34.3
Grande Anse	425.88	0.59	4.31×10^{-1}	46.31	0.68	0.09	53.70	1.27	0.35	27.2
Nippes	311.50	0.09	2.84×10^{-4}	8.86	0.96	0.21	91.15	1.06	0.21	6.9
Nord	970.50	0.16	7.79×10^{-2}	10.24	1.37	0.24	89.76	1.53	0.23	44.4
Nord Ouest	662.78	0.20	2.56×10^{-4}	14.26	1.20	0.11	85.74	1.40	0.11	36.4
Nord Est	358.28	0.22	1.43×10^{-3}	14.99	1.22	0.21	85.01	1.44	0.21	38.9
Ouest**[Ouest]	1187.83	0.45	2.04×10^{-4}	37.67	0.74	0.16	62.33	1.18	0.16	19.9
Port-au-Prince[Ouest]	2476.79	0.74	3.68×10^{-4}	39.27	1.15	0.13	60.73	1.89	0.13	60.5
Sud	704.76	0.21	1.32×10^{-3}	14.65	1.23	0.19	85.36	1.44	0.19	39.5
Sud Est	575.29	0.13	2.31×10^{-4}	11.11	1.04	0.14	88.89	1.17	0.14	18.3
Ouest	3664.62	0.43	1.78×10^{-3}	25.41	1.30	0.30	74.75	1.73	0.30	54.2

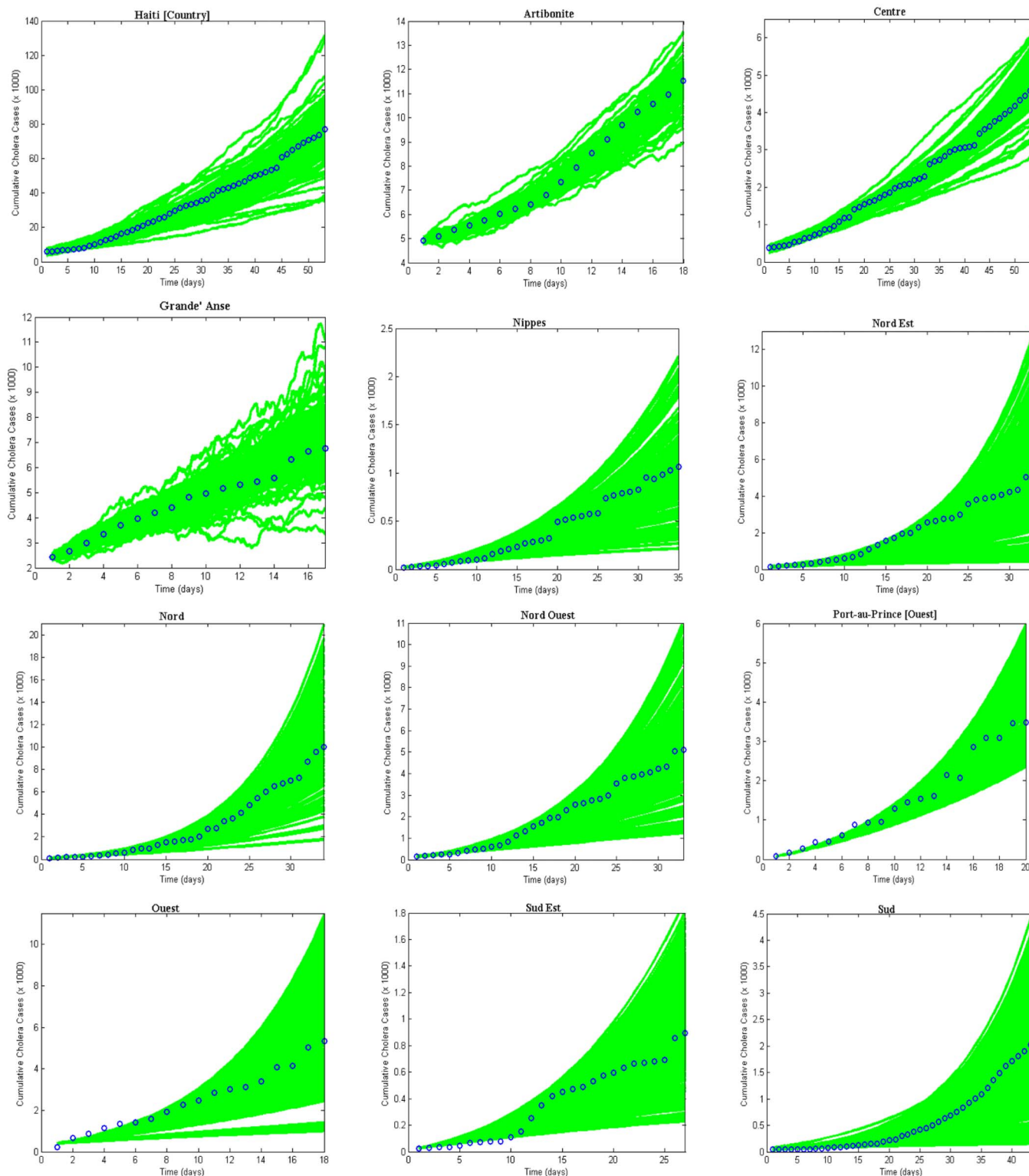


Figure 1 | Cholera model fitting for the cumulative cholera cases where the bold green lines represent the model fit and the blue circles mark the reported data for the cumulative number of cholera cases in the departments for 1000 runs.

infectious dose (with bicarbonate, or food) demonstrated among North American volunteers^{19,20}, we note that \mathcal{R}_0 estimates will change by less than 1%. However, these estimates will change by about 13% in vibrio concentration ranging from 1.5×10^9 to 10^{11} cells/ml. In Figure 4 we present sensitivity analysis results on the effects of χ on \mathcal{R}_0 estimates by plotting estimated \mathcal{R}_0 and corresponding values of χ . This parameter may be influenced by a number

of socio-economic factors, including adequacy of sewage disposal, and consequently may vary within communities. The distribution of exposure doses would be, in all likelihood, highly skewed. In Figure 4, we note that a change in χ from 1 to 100 only affects our estimates by approximately 3%. Thus, while there may be uncertainty around estimates for κ and χ , changes in these parameters do not substantially affect our results. The discontinuities in Figures 3 and 4 explain



Table 3 | Sensitivity analysis of vaccination efficacies from 50%–100% and the corresponding percentage coverage's in the departments and the whole country. Ouest department includes Port-au-Prince and Ouest** hospitalized cases

Department	Vaccination Coverage (%) Resulting in $\mathcal{R}_0 < 1$										
	50%	55%	60%	65%	70%	75%	80%	85%	90%	95%	100%
Haiti [Country]	70.8	64.4	59.0	54.5	50.6	47.2	44.2	41.6	39.3	37.3	35.4
Artibonite	>100	>100	>100	95.4	88.6	82.7	77.5	72.9	68.9	65.3	62.0
Centre	53.6	48.7	44.6	41.2	38.3	35.7	33.5	31.5	29.8	28.2	26.8
Grande Anse	42.4	38.6	35.4	32.6	30.3	28.3	26.5	25.0	23.6	22.3	21.2
Nippes	10.7	9.8	8.9	8.3	7.7	7.2	6.7	6.3	6.0	5.6	5.4
Nord	69.2	62.9	57.7	53.2	49.4	46.1	43.3	40.7	38.5	36.4	34.6
Nord Ouest	56.8	51.6	47.3	43.7	40.5	37.8	35.5	33.4	31.5	29.9	28.4
Nord Est	60.6	55.1	50.5	46.7	43.3	40.4	37.9	35.7	33.7	31.9	30.3
Ouest**[Ouest]	31.1	28.2	25.9	23.9	22.2	20.7	19.4	18.3	17.3	16.3	15.5
Port-au-Prince [Ouest]	94.4	85.8	78.7	72.6	67.4	62.9	59.0	55.5	52.5	49.7	47.2
Sud	61.6	56.0	51.3	47.4	44.0	41.1	38.5	36.2	34.2	32.4	30.8
Sud Est	28.6	26.0	23.9	22.0	20.4	19.1	17.9	16.8	15.9	15.1	14.3
Ouest	84.6	76.9	70.5	65.1	60.4	56.4	52.9	49.7	47.0	44.5	42.3

points where the curves stops being sensitive to changes in the parameters and the fitting procedure abruptly switches to favor the \mathcal{R}_h component.

In addition, we also explored the effects of other forms of unreported cholera infection such as asymptomatic colonization on \mathcal{R}_0 by assuming that the current data represent a certain percentage of reported cases in the clinical spectrum of cholera infection, and then fitting the model to Haitian data. Here, we extend our basic cholera model to incorporate a class of cholera asymptomatic cases as a proportion of total infections. We fit cholera reported data to the

class of symptomatic cases in the model based on the assumption that the available reported data only represent a percentage of the total cholera cases. This model also assumes that asymptomatic patients, who shed approximately 10^3 vibrios per gram of stool for only one day, do not significantly contribute to cholera infection²¹. Studies in the early 1970s suggested infection with cholera strains of classical biotype (responsible for the sixth cholera pandemic) resulted in severe cholera cases in only 11% of total infections; 59% of infections were asymptomatic and the remainder represented illness of mild to moderate severity. Other studies during the same period showed that

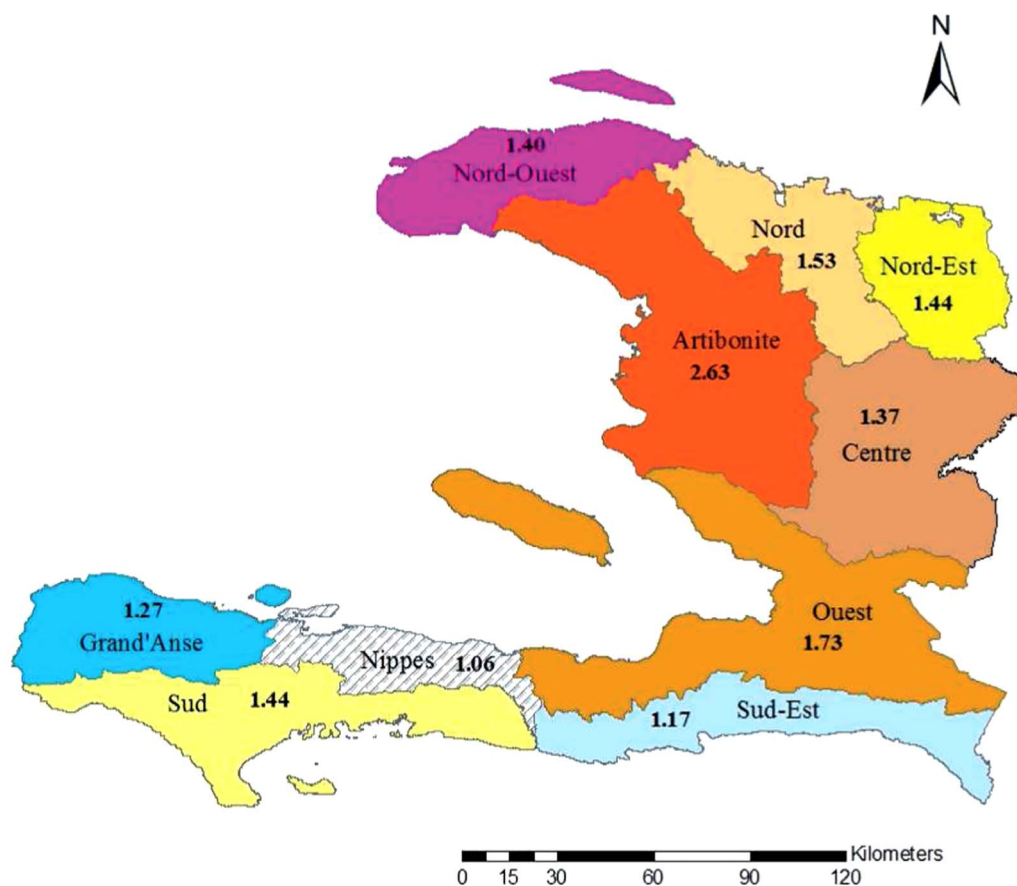


Figure 2 | Map of Haiti showing corresponding \mathcal{R}_0 values in the departments.

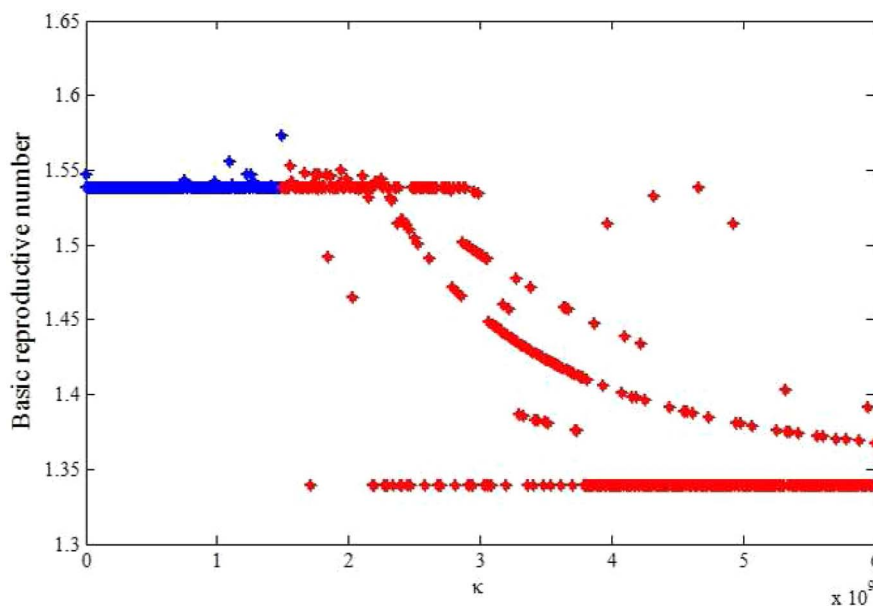


Figure 3 | The relationship between the basic reproductive number estimate (\mathcal{R}_0) and κ using aggregated data for Haiti using population sizes in Table 2 and parameter values in Table 4. The blue line denotes range of κ from 10^5 to 1.5×10^9 cells/ml and the red line denotes range range of κ from 1.5×10^9 to 10^{11} cells/ml (here our scale only shows 1.5×10^9 to 10^{10}).

only 2% infected with seventh pandemic biotype El Tor strains had severe disease, and 75% of infected persons were asymptomatic^{22,23}. However; recent studies have noted substantial increases in the percentage of patients with severe dehydration²⁴, and the percentage of asymptomatic infected patients appears to be much smaller (<50%, in a recent study by Harris *et al.* in Bangladesh²⁵), attributed to genetic changes in the organism^{26,27}. Based on these studies we carried out sensitivity analysis to assess the effects of varying the

percentage composition of reported symptomatic cases in the range 15–100% on the basic reproductive number. The range of the percentage composition of reported symptomatic cases (15–100%) considered here is consistent with recent findings which suggest an increase in the percentage of severe cases²⁴ and a smaller percentage of asymptomatic carriage (<50%)²⁵. The results in Figure 5 show that incorporating other forms of unreported cholera infection into the model changed \mathcal{R}_0 estimate by less than 5%.

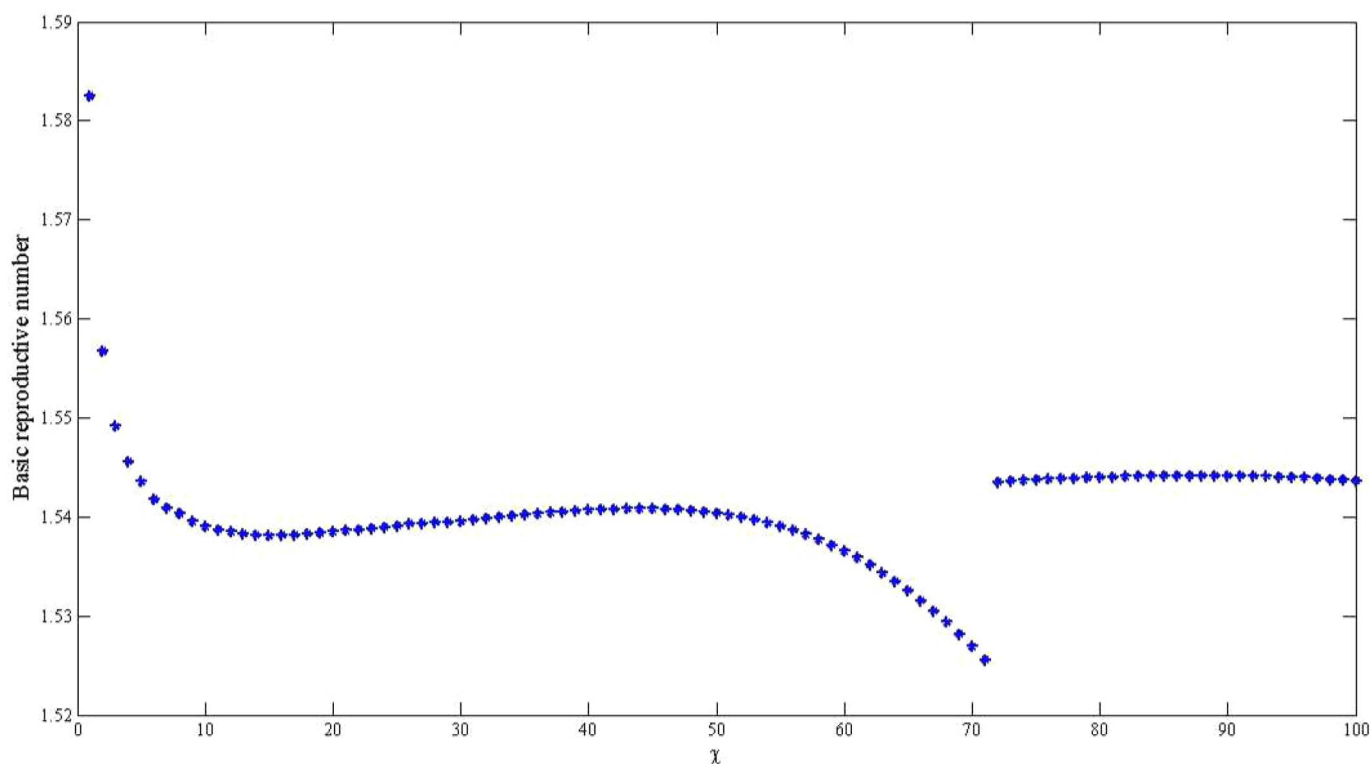


Figure 4 | The relationship between the basic reproductive number estimate (\mathcal{R}_0) and χ using aggregated data for Haiti using population sizes in Table 2 and parameter values in Table 4 and varying χ from 1 to 100.

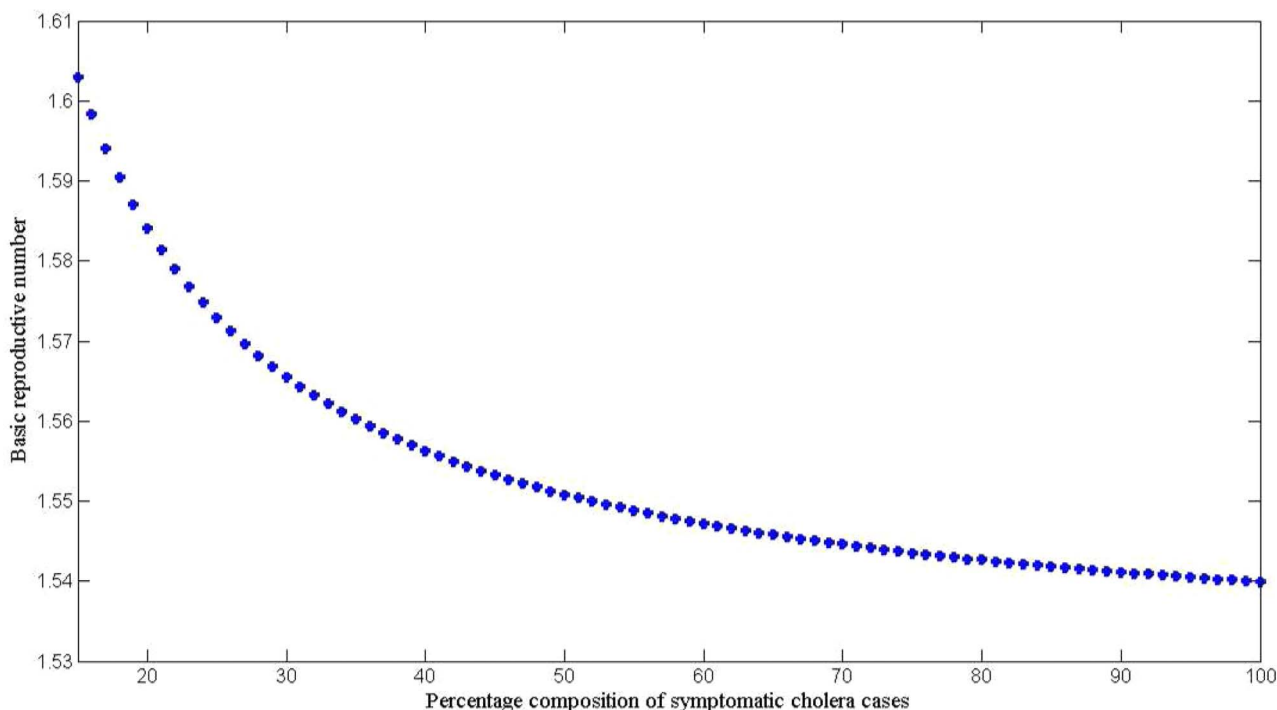


Figure 5 | The relationship between \mathcal{R}_0 and the percentage composition of reported symptomatic cholera cases reported using aggregated data for Haiti, parameter values from Table 4, and population size from Table 2.

Discussion

Estimated basic reproductive numbers varied across the departments ranging from 1.06 to 2.63. With the exception of the work by Chunara *et al.*²⁸, these results are in the same general range as the estimates from other mathematical models of the initial Haitian epidemic (Table 1), and are similar to those obtained for the 2008–2009 Zimbabwe outbreak⁶. However, in our model partial reproductive numbers were also highly heterogeneous suggesting that the patterns of transmission and transmission routes varied by department, and that some departments would be more amenable to vaccination compared with other kinds of interventions. The results in Table 2 suggest that on average, human-to-human transmission accounted for 68% of all the transmission, but both transmission pathways

contributed to initiating and sustaining cholera outbreaks across the departments. These quantities of $\mathcal{R}_0 > 1$ obtained for the departments and the whole country (see Table 2) suggest that future epidemics are highly likely, after population immunity has waned, unless effective control measures are put in place. These patterns address the concern that cholera may become endemic in Haiti because of a combination of a large estuarine system which may act as possible long-term ecological reservoirs for cholera, combined with continued transmission within human populations. In this setting, there would appear to be clear utility in mass vaccination with cholera vaccine with even moderate uptake, particularly in light of the significant herd protection afforded neighboring non-vaccinated individuals noted in prior studies²⁹. However, to achieve optimal

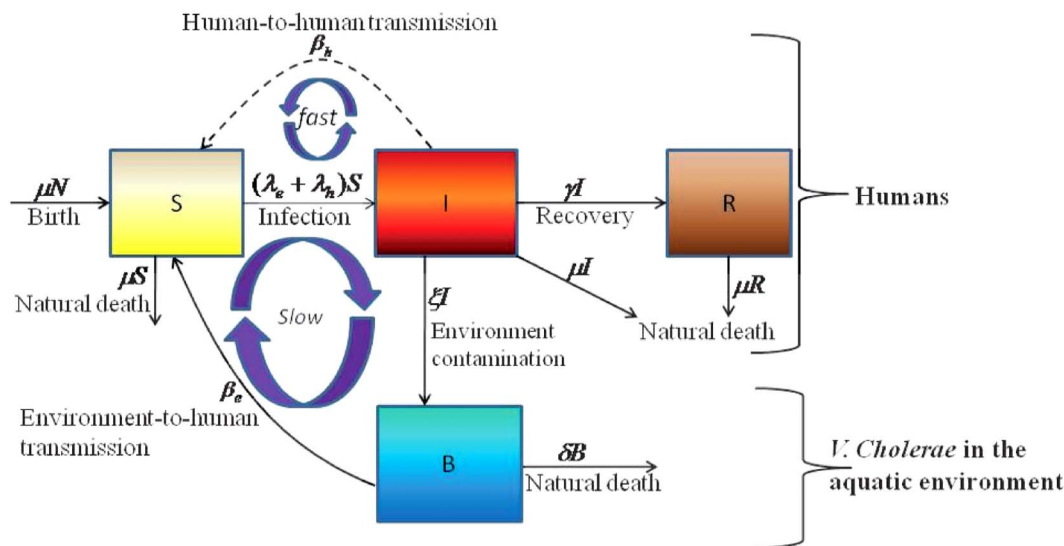


Figure 6 | Model flow diagram.



Table 4 | Cholera model parameters and values

Parameter	Symbol	Value	Source
Natural human birth and death rate	μ	61.2 years	35
Concentration of <i>V. cholerae</i> in the environment	κ	10^6 cells/ml	36
Rate of contribution to <i>V. cholerae</i> in the aquatic environment	χ	10 cells/ml-day/person	36
Rate of recovery from cholera	γ	(5 day) ⁻¹	37
Death rate of vibrios in the environment	δ	(30 day) ⁻¹	37

protection of the population, vaccination would need to be combined with other measures that permanently improve water systems and/or otherwise decrease the risk of transmission from environmental sources.

As alluded to above, the Haitian cholera epidemic has resulted in the development of several mathematical models (Table 1), driven, in part, by the close proximity of Haiti to the United States (with resultant interest in the outbreak), as well as recent developments in modeling techniques. The prediction of the sequence and timing of regional cholera epidemics in Haiti using a spatial approach was reported by Tuite *et al.*³. A similar spatial transmission model considering hydrologic and human mobility drivers of pathogen dispersal was proposed by Bertuzzo *et al.*⁴. Chao *et al.*⁵ used an individual, agent-based, dynamic transmission model to understand the dynamics of the cholera epidemic in Haiti. Not unexpectedly, these and other models have given somewhat different results (Table 1). Nonetheless, the range of values for \mathfrak{R}_0 has been fairly consistent; there is also clear convergence in the models related to the importance of vaccination, combined, potentially, with efforts to minimize transmission from environmental sources. The Haiti situation provides a unique opportunity to apply modeling results in development and implementation of practical public health interventions. As the history of cholera plays out in Haiti, it will be important to use the actual outcomes of these interventions to appropriately parameterize and assess the value of this and other models and modeling approaches.

Methods

The cholera model compartmentalizes the human population (Figure 6), of density N , into susceptibles S , infected I and recovered R (see on-line supplemental material included with reference⁶ for a complete mathematical description of the model). The concentration of vibrios in contaminated water is denoted by B . As previously described in application of the model to the Zimbabwe cholera epidemic of 2008–09, susceptible individuals acquire cholera infection either by ingesting environmental vibrios from contaminated aquatic reservoirs (a “slow” transmission route requiring a higher infectious dose) or through close contact with infected humans associated with ingestion of “hyperinfectious” vibrios^{30,31} (a “fast” transmission route related to the observed decrease in infectious dose seen among *V. cholerae* within a matter of hours of passage in diarrheal stool) at daily per-capita rates $\lambda_e = \frac{\beta_e B}{\kappa + B}$ and $\lambda_h = \beta_h I$ respectively, with the subscripts e and h denoting environment-to-human and human-to-human transmission routes. The constant κ is a shape parameter that determines the human infectious dose: when B equals κ the probability of ingestion resulting in human disease is 0.5. β_e and β_h are rates of exposure to vibrios from the contaminated environment and through human-to-human interaction respectively. Infected individuals recover from infection at a rate γ . Cholera infected individuals contribute to *V. cholerae* in the aquatic environment at a daily rate χ and vibrios have a net death rate δ in the environment. Readers interested in the model formulation, parameters and other properties should refer to^{6,23}. The resulting model as a system of coupled stochastic differential equations is as follows.

$$\begin{aligned}
 \frac{dS}{dt} &= \mu N - \beta_e(1 + \alpha_1 \xi_1(t))S \frac{B}{\kappa + B} - \beta_h(1 + \alpha_2 \xi_2(t))SI - \mu S, \\
 \frac{dI}{dt} &= \beta_e(1 + \alpha_1 \xi_1(t))S \frac{B}{\kappa + B} + \beta_h(1 + \alpha_2 \xi_2(t))SI - (\gamma + \mu)I, \\
 \frac{dR}{dt} &= \gamma I - \mu R, \\
 \frac{dB}{dt} &= \chi I - \delta B.
 \end{aligned} \tag{1}$$

Here, α_i for $i = 1, 2$ are real constants and $\xi(t) = (\xi_1(t), \xi_2(t))$ is the Gaussian white noise process to model environmental stochasticity satisfying $\langle \xi_i(t) \rangle = 0$ where

$\langle \rangle$ denotes ensemble average. It can also be shown that a solution of model system (Eqs. 1) is Markovian if and only if the external noises are white. We have assumed the Stratonovich interpretation of stochastic differential equations (Eqs. 1), which conserves the ordinary rule of calculus and in this case the stochastic differential equations can be considered as an ensemble of ordinary differential equations^{32,33}. A code in MATLAB® (The Mathworks, Inc., Version 7.10.0.499, R2010a) was used to fit the stochastic model system (Eqs. 1) to data and estimate the basic reproductive number and standard error for a given number of iterations. The code uses a fourth order Runge–Kutta numerical scheme for numerical integration and the built-in MATLAB® least-squares fitting routine lsqcurvefit. In each iteration:

1. Two white noise time series, $\xi_1(t)$ and $\xi_2(t)$ were generated;
2. The fitting routine lsqcurvefit found the parameters that minimized the sum of squared errors, including initial conditions (S_0, I_0, R_0, B_0) and parameters α_1 and α_2 that scale the variance of ξ_1 and ξ_2 ;
3. The estimates were stored in a table.

This was repeated 1000 times. The means and standard errors of these parameter estimates are reported in Table 2.

We fit the cholera model system (Eqs.1) to cumulative hospitalized cholera cases to estimate the basic reproductive numbers and critical vaccination coverage levels for the geospatially localized cholera outbreaks in Haiti by using daily data on numbers of hospitalized cases published on the MSPPP website¹⁵. These data may well be underestimated due to the weak health system in Haiti. However, despite quality issues surrounding the data set, it presents the best currently available platform for quantifying the magnitude of the cholera outbreak in Haiti.

The basic reproductive number (\mathfrak{R}_0), is defined as a measure of the average number of secondary cases generated by a primary case. Understanding its magnitude and variation can help to identify cholera “hot spots” and in designing targeted surveillance programs. The two transmission routes of cholera are quantitatively described by partial reproductive numbers, \mathfrak{R}_e and \mathfrak{R}_h that describe new cases that arise from either the fast human-to-human or the slower environment-to-human transmission routes, respectively. In the fitting, we estimate β_e and β_h to match the reported hospitalized cases in each department and for the whole country with other parameter values fixed as given in Table 4 and calculate the corresponding values of \mathfrak{R}_e , \mathfrak{R}_h and \mathfrak{R}_0 . For each department, we use the data points for the number of days that maximize the basic reproductive number estimate at the onset of an outbreak (i.e. maximizing β_e and β_h), using data for the period from 30 October 2010 to 25 December 2010. The data sets used for the estimation of \mathfrak{R}_0 were obtained by systematically testing different subsets of data from the start of an outbreak. We also normalize our population data by 1000 thus computed estimates of β_e and β_h are per capita.

The corresponding minimum vaccination coverage s (c) for a cholera vaccine with 78% efficacy⁷ for the 10 departments and the whole country given are based on the formula in³⁴,

$$c \geq \frac{1 - \mathfrak{R}_0^{-1}}{1 - (1-r)(1-s)} \tag{2}$$

where r is the fractional of the vaccinated population who are completely immunized and s is the proportional reduction of the susceptibility for those partially immunized.

1. CDC, Haiti cholera outbreak, <http://www.cdc.gov/haiticholera/situation/>, Accessed February 10 (2011).
2. Andrews, J. R. & Basu, S. Transmission dynamics and control of cholera in Haiti: an epidemic model. *Lancet* **377**, 1248–1255 (2011).
3. Tuite, A. L. *et al.* Cholera epidemic in Haiti, 2010: Using a transmission model to explain spatial spread of disease and identify optimal control interventions. *Ann. Intern. Med.* **154**, 293–302 (2011).
4. Bertuzzo, E. *et al.* Prediction of the spatial evolution and effects of control measures for the unfolding Haiti cholera outbreak. *Geophysical Research Letters* **38**, L06403 (2011).
5. Chao, D. L., Halloran, M. E. & Longini, I. M. Vaccination strategies for epidemic cholera in Haiti with implications for the developing world. *Proc. Natl. Acad. Sci. USA* **108**, 7081–7085 (2011).
6. Mukandavire, Z. *et al.* Estimating the reproductive numbers for the 2008–2009 cholera outbreaks in Zimbabwe. *Proc. Natl. Acad. Sci. USA* **108**, 8767–8772 (2011).
7. Lucas, M. E. *et al.* Effectiveness of mass oral cholera vaccination in Beira, Mozambique. *N. Engl. J. Med.* **352**, 757–767 (2005).
8. Piarroux, R. *et al.* Understanding the cholera epidemic, Haiti. *Emerg. Infect. Dis.* **17** (2011).



9. Sur, D. *et al.* Efficacy and safety of a modified killed-whole-cell oral cholera vaccine in India: an interim analysis of a cluster-randomised, double-blind, placebo-controlled trial. *Lancet* **374**, 1694–1702 (2009).
10. Thiem, V. D. *et al.* Long-term effectiveness against cholera of oral killed whole-cell vaccine produced in Vietnam. *Vaccine* **24**, 4297–4303 (2006).
11. Clemens, J. D. *et al.* Field trial of oral cholera vaccines in Bangladesh: results from three-year follow-up. *Lancet* **335**, 270–273 (1990).
12. Clemens, J. D. *et al.* Cross-protection by B subunit whole cell cholera vaccine against diarrhea associated with heat-labile toxin-producing enterotoxigenic *Escherichia coli*: results of a large-scale field trial. *J. Infect. Dis.* **158**, 372–377 (1988).
13. Date, K. A. *et al.* Consideration for oral cholera vaccine use during outbreak after earthquake in Haiti, 2010–2011. *Emerg. Infect. Dis.* **17** (2011)
14. Sanchez, J. L. *et al.* Protective efficacy of oral whole-cell/recombinant-B-subunit cholera vaccine in Peruvian military recruits. *Lancet* **344**, 1273–1276 (1994).
15. MSPP website at: http://mspp.gouv.ht/site/index.php?option=com_content&view=article&id=57&Itemid=1, Accessed February 2 (2011).
16. Franco, A. A. *et al.* Cholera in Lima, Peru, correlates with prior isolation of *Vibrio cholerae* from the environment. *Am. J. Epidemiol.* **146**, 1067–1075 (1997).
17. Huq, A. *et al.* Critical factors influencing the occurrence of *Vibrio cholerae* in the environment in Bangladesh. *Appl. Environ. Microbiol.* **71**, 4645–4654 (2005).
18. Kaper, J. B., Morris, J. G. Jr. & Levine, M. M. Cholera. *Microbiol. Rev.* **8**, 48–86 (1995).
19. Cash, R. A. *et al.* Response of man to infection with *Vibrio cholerae*. I. Clinical, serologic, and bacteriologic responses to a known inoculum. *J. Infect. Dis.* **129**, 45–52 (1974).
20. Levine, M. M. *et al.* Volunteer studies in development of vaccines against cholera and enterotoxigenic *Escherichia coli*: A review. In: Holme T, Holmgren J, Merson MH, Mollby R. *Acute Enteric Infections in Children. New Prospects for Treatment and Prevention*. Elsevier/NorthHolland Biomedical Press, pp 443–459 (1981).
21. Mosley, W. H., Ahmad, S., Benenson, A. S. & Ahmed, A. The relationship of vibriocidal antibody titre to susceptibility to cholera in family contacts of cholera patients. *Bull. World Health Organ.* **38**, 777–785 (1968).
22. Gangarosa, E. J. & Mosley, W. H. *Epidemiology and surveillance of cholera*. In: Barua, D., Burrows, W., editors. *Cholera*. Philadelphia: W. B. Saunders, pp 381–403 (1974).
23. Morris, J. G. Jr. Cholera: Modern pandemic disease of ancient lineage. *Emerg. Infect. Dis.* **17**, (2011).
24. Siddique, A. K. *et al.* El Tor cholera with severe disease: a new threat to Asia and beyond. *Epidemiol. Infect.* **138**, 347–352 (2010).
25. Harris, J. B. *et al.* Susceptibility to *Vibrio cholerae* infection in a cohort of household contacts of patients with cholera in Bangladesh. *PLoS Negl. Trop. Dis.* **2**, e221 (2008).
26. Nair, G. B. *et al.* New variants of *Vibrio cholerae* O1 biotype El Tor with attributes of the classical biotype from hospitalized patients with acute diarrhea in Bangladesh. *J Clin Microbiol.* **40**, 3296–3299 (2002).
27. Safa, A., Nair, G. B. & Kong, R. Y. C. Evolution of new variants of *Vibrio cholerae* O1. *Trends Microbiol.* **18**, 46–54 (2010).
28. Chunara, R., Andrews, J. R. & Brownstein, J. S. Social and news media enable estimation of epidemiological patterns early in the 2010 Haitian cholera outbreak. *Am. J. Trop. Med. Hyg.* **86**, 39–45 (2012).
29. Ali, M. *et al.* Herd immunity conferred by killed oral cholera vaccines in Bangladesh: a reanalysis. *Lancet* **366**, 44–49 (2005).
30. Merrell, D. S. *et al.* Host-induced epidemic spread of the cholera bacterium. *Nature* **417**, 642–645 (2002).
31. Nelson, E. J., Harris, J. B., Morris, Jr. J. G., Calderwood, S. B. & Camilli, A. Cholera transmission: the host, pathogen and bacteriophage dynamic. *Nat. Rev. Microbiol.* **7**, 693–702 (2009).
32. Øksendal, B. *Stochastic Differential Equations: An Introduction with Applications*, (Springer, New York, 1998), 5th edn.
33. Samanta, G. P. The effect of random fluctuating environment on interacting species with time delay. *Int. J. Math. Educ. Sci. Technol.* **27**, 13–21 (1996).
34. Dietz, K. The estimation of the basic reproduction number for infectious diseases. *Statistical Methods in Medical Research* **2**, 23–41 (1993).
35. UN data, A world of information, <http://data.un.org/Data.aspx?q=haiti&d=PopDiv&f=variableID%3A68%3BcrID%3A332>. Accessed March 1 (2011).
36. Codeço, C. T. Endemic and epidemic dynamics of cholera: The role of the aquatic reservoir. *BMJ Infect. Dis.* **1** (2001).
37. Hartley, D. M., Morris, Jr. J. G. & Smith, D. L. Hyperinfectivity: A Critical Element in the Ability of *V. cholerae* to Cause Epidemics? *PLoS Med.* **3**, e7 (2006).

Acknowledgments

Z.M. and J.G.M. are supported in part by a grant from the National Institute of Allergy and Infectious Diseases (RO1AI097405, awarded to J.G.M.). Z.M. is also supported by the UF Science for Life Program, an interdisciplinary program with support from the Howard Hughes Medical Institute. D.L.S. is funded by the RAPIDD program of the Science and Technology Directorate, Department of Homeland Security, and the Fogarty International Center, National Institutes of Health. The authors acknowledge Nathaniel Hupert, Michael L. Washington and their colleagues at the U.S. Centers for Disease Control and Prevention's Preparedness Modeling Unit and the group of modelers involved in the useful discussions on the cholera outbreak in Haiti.

Author contributions

Dr. Mukandavire was responsible for construction of the model and initial manuscript preparation. Drs. Smith and Morris assisted with conceptualization of the project and preparation of the manuscript.

Additional information

Competing financial interests: The authors declare no competing financial interests.

License: This work is licensed under a Creative Commons Attribution-NonCommercial-NoDerivs 3.0 Unported License. To view a copy of this license, visit <http://creativecommons.org/licenses/by-nc-nd/3.0/>

How to cite this article: Mukandavire, Z., Smith, D.L. & Morris, J.G. Jr. Cholera in Haiti: Reproductive numbers and vaccination coverage estimates. *Sci. Rep.* **3**, 997; DOI:10.1038/srep00997 (2013).